Model-Free Sliding-Mode Controller for
Soft Landing of Reluctance Actuators

Eduardo Moya-Lasheras * **Edgar Ramirez-Laboreo** *
Carlos Sagues *

* *Departamento de Informatica e Ingenieria de Sistemas (DIIS) and*
Instituto de Investigacion en Ingenieria de Aragon (I3A),
Universidad de Zaragoza, Zaragoza 50018, Spain,
(e-mail: emoya@unizar.es, ramirlab@unizar.es, csagues@unizar.es)

Abstract: Some electromagnetic actuators suffer from high velocity impacts during non-controlled switching operations, which cause contact bouncing, mechanical wear, and acoustic noise. Soft-landing control strategies aim at minimizing the impact velocities of these devices to improve their performance. This paper presents a sliding-mode controller for soft landing of single-coil reluctance actuators. It is a switching model-free controller, which results in a very simple implementation. A generalized dynamical hybrid model of an actuator is utilized for deriving the robustness condition, based on the Lyapunov theory. Then, the condition is evaluated for a dynamical model, based on a commercial device, and several reference trajectories. Finally, the controller performance is validated through simulations. The effect of the sampling rate on the resulting impact velocities is also analyzed.

Keywords: Actuators, Electromagnetic devices, Modeling, Nonlinear control, Robust control, Sliding-mode control, Tracking

1. INTRODUCTION

A reluctance actuator is a type of nonlinear electromechanical device which generates a reluctance-based magnetic force to move its armature. Particularly, single-coil actuators are used in an extensive variety of industrial applications because of their fast response, compactness, high energy efficiency, and low cost. Thus, there is a great research interest concerning modeling, identification, estimation, and control of this class of actuators.

Regarding the control, one of the main motivations and challenges is to achieve soft landing during switching operations; thus reducing contact bouncing, impact noise and mechanical wear. In the literature, there are several control proposals for reluctance actuators, e.g., based on the backstepping technique (Kahveci and Kolmanovsky, 2010), energy compensation (Yang et al., 2013), a linearization method (Katalenic et al., 2016), or cycle-to-cycle adaptation (Moya-Lasheras et al., 2019), among others.

One important drawback of many mass-market single-coil reluctance actuators is the manufacturing variability among devices from the same ensemble. Moreover, the identification of every unit may impose a prohibitive cost. One major approach to deal with model uncertainties is the sliding-mode control (SMC) theory (Slotine and Li, 1991). There are several works that take this approach. Most commonly, the control law is divided into two terms:

an equivalent and a switching control term (Lee et al., 2015; Zhao et al., 2016). Alternatively, Eyabi and Washington (2006) proposed a SMC with only a switching term, which is then approximated to a proportional one. One important aspect that is omitted in these works is the definition of the tracking trajectory, which directly affects the robustness conditions for the SMC. Another important issue is the influence of the sampling rate. In general, the sliding accuracy is proportional to the square of the switching delay (Levant, 1993). Still, its effect on the resulting impact velocities needs to be evaluated.

This paper presents a robust SMC controller for single-coil reluctance actuators. It is purely a switching controller, which results in a very simple and computationally inexpensive implementation. Although the resulting controller is model-free—i.e. it does not depend on any model functions or parameters—a dynamic model is required during the design process to guarantee its robustness. The generalized system, which presents both continuous and discrete dynamic behavior, is modeled with a hybrid automaton. A robustness condition is derived, which depends on the system dynamics and the position trajectory. It is then evaluated for a specific dynamic model, based on a commercial solenoid valve, and several trajectories. The first contribution of the paper is the proposal of a switching model-free SMC, which works for every discrete mode of the system. The second contribution is the analysis of the influence of the sampling rate on the impact velocities.

2. SYSTEM DYNAMICS

A general single-coil reluctance actuator is represented in Fig. 1. The magnetic core is divided into two parts: a fixed
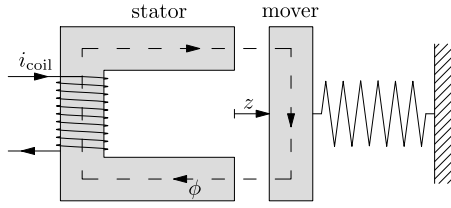
Fig. 1. Schematic representation of a single-coil reluctance actuator.

part (stator) and a movable part (mover or armature). The air gap between them is dependent on the position of the mover. There are two types of operations depending on the direction of the movement: in a making operation, the magnetic force is large enough to attract the mover toward the stator; whereas in a breaking operation, the magnetic force is reduced and the passive forces (e.g. elastic or gravity) move the armature in the opposite direction. Moreover, the position of the mover is restricted between a lower and an upper limit.

The motion dynamics is given by Newton's second law, with two forces,

$$\dot{v} = f_v(z, v, \phi) = \frac{1}{m} \left(F_{\text{pas}}(z, v) + F_{\text{mag}}(z, \phi) \right), \quad (1)$$

where z, v, and $\dot{v}$ are the position, velocity and acceleration of the mover; F_{pas}, and F_{mag} are the passive and magnetic forces; ϕ is the magnetic flux; and m is the moving mass. Note that the dynamic function of v is expressed compactly as f_v. The force that can be controlled—albeit indirectly—is F_{mag}, which is defined as (Ramirez-Laboreo et al., 2016)

$$F_{\text{mag}} = -\frac{1}{2} \mathcal{R}'_{\text{g}}(z) \phi^2, \qquad \mathcal{R}'_{\text{g}}(z) = \frac{\partial \mathcal{R}_{\text{g}}(z)}{\partial z}, \quad (2)$$

where $\mathcal{R}_{\text{g}}$ is the gap reluctance. Note that $\mathcal{R}'_{\text{g}} > 0$, and therefore $F_{\text{mag}} \leq 0$, for all $z \in [z_{\min}, z_{\max}]$ (i.e. the magnetic force is always attractive).

Then, ϕ can be related to the current through the coil i_{coil} in terms of the total reluctance, given Ampère's circuital law,

$$N \, i_{\text{coil}} + i_{\text{eddy}} = \left(\mathcal{R}_{\text{c}}(\phi) + \mathcal{R}_{\text{g}}(z) \right) \phi, \quad (3)$$

where N is the number of coil turns, $\mathcal{R}_{\text{c}}$ is the core reluctance, and i_{eddy} is the net eddy current through the core. Assuming that the magnetic flux density is constant across the section, i_{eddy} is proportional to the magnetic flux derivative (Ramirez-Laboreo et al., 2019),

$$i_{\text{eddy}} = -k_{\text{e}} \, \dot{\phi}. \quad (4)$$

Most commonly, the voltage is treated as the system input u, because it can be directly supplied to the device. The dynamics of the magnetic flux is given by the electrical circuit equation,

$$u = R \, i_{\text{coil}} + N \, \dot{\phi}, \quad (5)$$

where R is the coil resistance. Then, substituting (3) into (5) and solving for $\dot{\phi}$, the dynamic function is derived as

$$
\begin{aligned}
\dot{\phi} &= f_\phi(z, \phi) + B_\phi \, u \\
&= -\frac{R \left(\mathcal{R}_{\text{g}}(z) + \mathcal{R}_{\text{c}}(\phi) \right) \phi}{N^2 + R \, k_{\text{e}}} + \frac{N}{N^2 + R \, k_{\text{e}}} \, u, \quad (6)
\end{aligned}
$$

where the function f_ϕ depends on the position and magnetic flux, and B_ϕ is a constant.
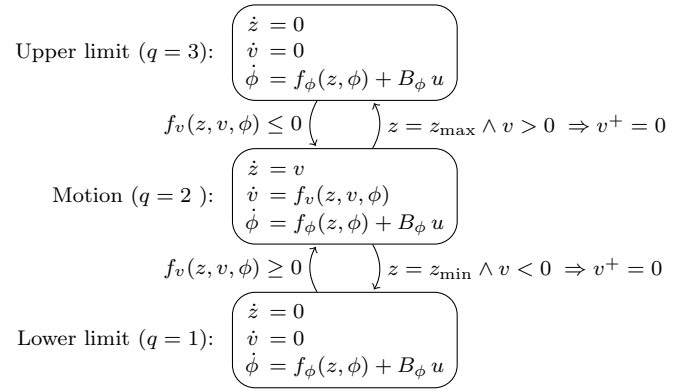

Fig. 2. Hybrid automaton that models the dynamics of reluctance actuators with a limited range of motion.

The complete system dynamics can be described through a state-space representation with three state variables (z, v, and ϕ). As the motion is constrained, z and v must be static if the mover reaches one of the two limits. Thus, the system is modeled with a hybrid automaton, with three discrete modes, as illustrated in Fig. 2. Each transition is accompanied by its guard condition. There is also a reset function when transitioning to one of the position limits: $v^+ = 0$.

3. CONTROL DESIGN

3.1 Trajectory planning

The first critical aspect of the soft-landing tracking control is the definition of the position trajectory z_{ref}, for all time $t \in [t_0, t_{\text{f}}]$. For a given operation, the initial position is z_0 and the desired final position is z_{f}.

Let t_{land} be the intended instant in which the armature reaches the final position. For a perfect soft landing, z_{ref} should satisfy

$$z_{\text{ref}}(t_{\text{land}}) = z_{\text{f}}, \quad v_{\text{ref}}(t_{\text{land}}) = 0, \quad a_{\text{ref}}(t_{\text{land}}) = 0, \quad (7)$$

where

$$v_{\text{ref}}(t) = \dot{z}_{\text{ref}}(t), \qquad a_{\text{ref}}(t) = \dot{v}_{\text{ref}}(t). \quad (8)$$

Equivalently, in order to start the motion smoothly, z_{ref} should satisfy

$$z_{\text{ref}}(t_{\text{takeoff}}) = z_0, \quad v_{\text{ref}}(t_{\text{takeoff}}) = 0, \quad a_{\text{ref}}(t_{\text{takeoff}}) = 0, \quad (9)$$

where t_{takeoff} is the take-off instant.

During motion ($q = 2$), the acceleration is determined from (1). Therefore, in order to start moving immediately at $t = t_{\text{takeoff}}$, ϕ should be ϕ_{takeoff}, such that $f_v(z_0, 0, \phi_{\text{takeoff}}) = 0$. Note that there are two symmetrical solutions of ϕ_{takeoff} (positive and negative), because f_v is an even function with respect to ϕ. Note also that the controller should decrease $|\phi|$ if $q = 1$, or increase it if $q = 3$, until it reaches ϕ_{takeoff}. Thus, prior to moving, a static interval is defined,

$$z_{\text{ref}}(t) = z_0, \quad \forall t \in [t_0, t_{\text{takeoff}}]. \quad (10)$$

where $t_{\text{takeoff}} - t_0$ should be large enough to let the magnetic flux reach ϕ_{takeoff} before t_{takeoff}.

In the second interval (from t_{takeoff} to t_{land}), a position trajectory must be defined to reach z_{f} smoothly. Thus, z_{ref} should be a function of time t, for all $t \in [t_{\text{takeoff}}, t_{\text{land}}]$,

with boundary conditions (9) and (7). In the third interval (from t_{land} to t_{f}), the mover must be kept in the desired final position, so

$$z_{\text{ref}}(t) = z_{\text{f}}, \quad \forall t \in [t_{\text{land}}, t_{\text{f}}]. \tag{11}$$

Once a trajectory is defined, its feasibility should be checked. First, the position must be kept inside its bounds,

$$z_{\text{ref}}(t) \in [z_{\min}, z_{\max}], \quad \forall t. \tag{12}$$

Secondly, the required magnetic force F_{mag}^* should be calculated, and ensure that it is always nonpositive, because repelling magnetic forces are not physically possible (see (2)),

$$F_{\text{mag}}^*(t) = m\, a_{\text{ref}}(t) - F_{\text{pas}}(z_{\text{ref}}(t), v_{\text{ref}}(t)) \le 0, \quad \forall t. \tag{13}$$

Moreover, magnetic saturation must also be taken into account. Given the saturated value of the magnetic flux ϕ_{sat}, the required magnetic force should also satisfy

$$F_{\text{mag}}^*(t) \ge -\frac{1}{2} \mathcal{R}_{\text{g}}'(z_{\text{ref}}(t))\, \phi_{\text{sat}}^2, \quad \forall t. \tag{14}$$

3.2 Control for motion dynamics

The controller is initially designed based on the dynamic equations of the motion mode ($q = 2$), which can be expressed compactly as

$$\dot{\boldsymbol{x}} = \boldsymbol{f}(\boldsymbol{x}) + \boldsymbol{B}\, u, \tag{15}$$

where

$$\boldsymbol{x} = \begin{bmatrix} z \\ v \\ \phi \end{bmatrix}^{\mathsf{T}}, \quad \boldsymbol{f}(\boldsymbol{x}) = \begin{bmatrix} v \\ f_v(z, v, \phi) \\ f_\phi(z, \phi) \end{bmatrix}, \quad \boldsymbol{B} = \begin{bmatrix} 0 \\ 0 \\ B_\phi \end{bmatrix}. \tag{16}$$

As stated in the introduction, our proposal relies on an SMC. It is assumed that the position z, velocity v, and acceleration a can be obtained either through measurement or estimation. The proposed sliding surface is defined in terms of their errors,

$$\begin{aligned} s &= \left(\lambda_1 + \frac{\mathrm{d}}{\mathrm{d}t}\right)\left(\lambda_2 + \frac{\mathrm{d}}{\mathrm{d}t}\right)\tilde{z} \\ &= \tilde{a} + (\lambda_1 + \lambda_2)\,\tilde{v} + \lambda_1 \lambda_2\, \tilde{z}, \end{aligned} \tag{17}$$

where λ_1 and λ_2 are positive constants; and $\tilde{z}$, $\tilde{v}$, and $\tilde{a}$ are the position error and its derivatives,

$$\tilde{z} = z - z_{\text{ref}}, \qquad \tilde{v} = v - v_{\text{ref}}, \qquad \tilde{a} = a - a_{\text{ref}}. \tag{18}$$

To analyze the convergence to the sliding surface $s = 0$, the following Lyapunov function is defined,

$$V = \frac{1}{2}\, s^2. \tag{19}$$

Thus, to ensure that s converges to zero in finite time, we impose the following condition,

$$\dot{V} = s\, \dot{s} \le -\eta\, |s|, \tag{20}$$

where η is a strictly positive constant that determines the convergence speed ($|\dot{s}| \ge \eta$).

Then, by deriving (17) and substituting into (20),

$$\dot{V} = s\, \big(j - j_{\text{ref}} + (\lambda_1 + \lambda_2)\,\tilde{a} + \lambda_1 \lambda_2\, \tilde{v}\big), \tag{21}$$

where $j = \dot{a}$ is the jerk and $j_{\text{ref}} = \dot{a}_{\text{ref}}$ is the reference jerk. The jerk j can be derived from f_v and the dynamic equation (15) as

$$j = \frac{\mathrm{d}f_v(\boldsymbol{x})}{\mathrm{d}t} = \frac{\partial f_v(\boldsymbol{x})}{\partial \boldsymbol{x}}\, \boldsymbol{f}(\boldsymbol{x}) + \frac{\partial f_v(\boldsymbol{x})}{\partial \boldsymbol{x}}\, \boldsymbol{B}\, u. \tag{22}$$

Note that j depends on u. Thus, the convergence condition (20) can be expressed in terms of the control u,

$$s\, (f_j - j_{\text{ref}} + \varepsilon - B_j\, u) \le -\eta\, |s|, \tag{23}$$

where

$$\varepsilon = \varepsilon(\tilde{v}, \tilde{a}) = (\lambda_1 + \lambda_2)\,\tilde{a} + \lambda_1 \lambda_2\, \tilde{v}, \tag{24}$$

$$\begin{aligned} f_j = f_j(\boldsymbol{x}) &= \frac{\partial f_v(\boldsymbol{x})}{\partial \boldsymbol{x}}\, \boldsymbol{f}(\boldsymbol{x}) \\ &= \frac{1}{m}\left(\frac{\partial F_{\text{pas}}}{\partial z}(z, v)\, v + \frac{\partial F_{\text{pas}}}{\partial v}(z, v)\, a \right. \\ &\quad \left. -\frac{1}{2}\mathcal{R}_{\text{g}}''(z)\, \phi^2\, v - \mathcal{R}_{\text{g}}'(z)\, \phi\, f_\phi(z, \phi)\right), \end{aligned} \tag{25}$$

$$B_j = B_j(\boldsymbol{x}) = -\frac{\partial f_v(\boldsymbol{x})}{\partial \boldsymbol{x}}\, \boldsymbol{B} = \frac{\mathcal{R}_{\text{g}}'\, \phi\, B_\phi}{m}. \tag{26}$$

Then, with some manipulations,

$$\operatorname{sgn}(s)\, B_j\, u \ge \operatorname{sgn}(s)\, (f_j - j_{\text{ref}} + \varepsilon) + \eta. \tag{27}$$

Note that, assuming $\mathcal{R}_{\text{g}}' > 0$ for all $z \in [z_{\min}, z_{\max}]$, it is obtained that $\operatorname{sgn}(B_j) = \operatorname{sgn}(\phi)$. Thus, the control u must satisfy the following condition,

$$\operatorname{sgn}(s)\, \operatorname{sgn}(\phi)\, u \ge \frac{\operatorname{sgn}(s)\, (f_j - j_{\text{ref}} + \varepsilon) + \eta}{|B_j|}. \tag{28}$$

We propose this model-free control,

$$u_{\text{motion}} = u_{\max}\, \operatorname{sgn}(s)\, \operatorname{sgn}(\phi), \tag{29}$$

where $u_{\max}$ is a constant that, in order to ensure the convergence to $s = 0$, must satisfy

$$u_{\max} \ge \max\left(\frac{|f_j - j_{\text{ref}} + \varepsilon| + \eta}{|B_j|}\right). \tag{30}$$

3.3 Control for hybrid dynamics

In the previous section, we have proposed a controller and proved its convergence for the motion dynamics ($q = 2$). Now, we ensure that it works for the complete hybrid system. For that, we propose a slight modification of the Lyapunov function,

$$V = \frac{1}{2}\, \sigma^2, \tag{31}$$

where σ is a generalization of s. It is defined as

$$\sigma = f_v(z, v, \phi) - a_{\text{ref}} + (\lambda_1 + \lambda_2)\,\tilde{v} + \lambda_1 \lambda_2\, \tilde{z}. \tag{32}$$

Note that σ is equal to s in the case of motion, because $a = f_v$. On the other hand, before the start of motion ($t \le t_{\text{takeoff}}$), $\sigma = f_v$. Therefore, $\sigma = 0$ implies that $\phi = \phi_{\text{takeoff}}$. As a result, if $\sigma = 0$, the system behaves as desired both before and after the start of motion.

Following the same line of reasoning as in Section 3.2, convergence to $\sigma = 0$ requires

$$\operatorname{sgn}(\sigma)\, \operatorname{sgn}(\phi)\, u \ge \frac{\operatorname{sgn}(\sigma)\, (f_j - j_{\text{ref}} + \varepsilon) + \eta}{|B_j|}. \tag{33}$$

To keep the controller model-free, the proposal cannot depend on f_v. Instead, it should be a function of s. We generalize the proposed control (29),

$$u_{\text{hybrid}} = u_{\max}\, \operatorname{sgn}(\phi)\, \operatorname{sgn}^*(s), \tag{34}$$

where

$$\text{sgn}^*(s) = \begin{cases} -1, & \text{if } s < 0, \\ +1, & \text{if } s > 0, \\ -1, & \text{if } s = 0 \wedge q = 1, \\ +1, & \text{otherwise.} \end{cases} \tag{35}$$

Under the assumption that (30) is satisfied, a sufficient condition for convergence is

$$\text{sgn}^*(s) = \text{sgn}(\sigma). \tag{36}$$

Then, convergence is studied in three separate cases. First, if $q = 2$, the convergence condition is directly guaranteed because $s = \sigma$.

Secondly, if $z = z_{\text{ref}} = z_{\max}$ or $z = z_{\text{ref}} = z_{\min}$, s is always zero, but σ may be not. Note that $a_{\text{ref}} = \tilde{v} = \tilde{z} = 0$. Then,

$$\text{sgn}(\sigma) = \text{sgn}(f_v). \tag{37}$$

Note also that $f_v < 0$ if $q = 1$ and $f_v > 0$ if $q = 3$, otherwise the hybrid system would make a transition to $q = 2$ (see guard conditions in Fig. 2). Therefore,

$$\text{sgn}(\sigma) = \text{sgn}(f_v) = \begin{cases} -1, & \text{if } q = 1, \\ +1, & \text{if } q = 3. \end{cases} \tag{38}$$

Then, given the proposed definition of $\text{sgn}^*(s)$, condition (36) holds, so convergence is still guaranteed.

Thirdly, we still need to check the convergence of the controller in the case that the position is in one of the limits ($q \neq 2$), but the reference is not. In that event, (32) is simplified into

$$\sigma = f_v + s, \tag{39}$$

where

$$s = -a_{\text{ref}} - (\lambda_1 + \lambda_2)\, v_{\text{ref}} - \lambda_1 \lambda_2 \,(z - z_{\text{ref}}). \tag{40}$$

Assuming that the position trajectory is defined smoothly at the start of the movement, condition (36) is satisfied because, when $z_0 = z_{\min}$ (breaking operation),

$$f_v < 0 \qquad \text{and} \qquad (z_{\text{ref}} - z_0),\, v_{\text{ref}},\, a_{\text{ref}} \geq 0. \tag{41}$$

Equivalently, when $z_0 = z_{\max}$ (making operation),

$$f_v > 0, \qquad \text{and} \qquad (z_{\text{ref}} - z_0),\, v_{\text{ref}},\, a_{\text{ref}} \leq 0. \tag{42}$$

On the other hand, at the end of movement, if z has reached the limit but z_{ref} not yet, the condition is not necessarily satisfied. This may seem like a limitation but, if the mover has reached the final position prematurely, it is actually preferable to fix it instead of separating it to continue following the trajectory. Thus, expert rules are added to the controller so the mover is kept at $z_{\text{f}} = z_{\min}$ (making operation) or $z_{\text{f}} = z_{\max}$ (breaking operation),

$$u = \begin{cases} u_{\max}\, \text{sgn}(\phi) & \text{if } z = z_{\text{f}} = z_{\min}, \\ 0, & \text{if } z = z_{\text{f}} = z_{\max}, \\ u_{\max}\, \text{sgn}^*(s)\, \text{sgn}(\phi), & \text{otherwise.} \end{cases} \tag{43}$$

4. ANALYSIS AND DISCUSSION

4.1 Robustness analysis

For the given dynamic model, it is impossible to guarantee robustness in general, for any feasible state. As a clear counterexample, setting $\phi = 0$ makes $B_j = 0$, and $u_{\max} \geq \infty$ (see (30)). Therefore, the robustness must be studied for a given trajectory. To illustrate this, the robustness is analyzed for three different scenarios.
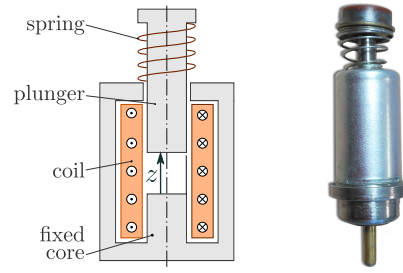

Fig. 3. Solenoid valve: schematic representation (left) and photo (right).

Table 1. Parameters of the solenoid valve.

Param.	Value		Param.	Value	
m	0.0016	kg	N	1200	
k_{s}	61.8	N/m	R	50	Ω
z_{s}	0.019	m	k_{e}	1630	Ω^{-1}
c	0.8	Ns/m	$\mathcal{R}_{\text{c},0}$	4.41×10^6	H^{-1}
$z_{\min}$	0	m	ϕ_{sat}	2.6×10^{-5}	Wb
$z_{\max}$	0.001	m			

Then, three position trajectories are defined. Each one of them consists of a making operation, followed by a breaking operation. The motion intervals are defined with a 5th degree polynomial, satisfying the boundary conditions (7), (9). Moreover, for the sake of simplicity, the time intervals are defined in terms of the motion duration (τ_{mov}),

$$t_{\text{land}} - t_{\text{takeoff}} = \tau_{\text{mov}}, \tag{44}$$
$$t_{\text{takeoff}} - t_0 = t_{\text{f}} - t_{\text{land}} = \tau_{\text{mov}}/4, \tag{45}$$

where τ_{mov} is 3, 4 or 5 ms, for each case.

The actuator model is particularized to a commercial solenoid valve, depicted in Fig. 3, whose estimated parameters are presented in Table 1. The passive force is generated by the spring and friction. It is modeled as a mass-spring-damper system,

$$F_{\text{pas}} = k_{\text{s}}\,(z_{\text{s}} - z) - c\,v, \tag{46}$$

where k_{s} is the spring constant, z_{s} is the spring resting position, and c is the damping coefficient. Moreover, the core reluctance is given by a parametric expression that takes into account magnetic saturation (Moya-Lasheras et al., 2017),

$$\mathcal{R}_{\text{c}} = \frac{\mathcal{R}_{\text{c},0}}{1 - \phi/\phi_{\text{sat}}}, \tag{47}$$

where $\mathcal{R}_{\text{c},0}$ is the core reluctance for $\phi = 0$, and ϕ_{sat} is the saturated value of the magnetic flux.

The gap reluctance, on the other hand, is highly nonlinear with respect to the position. Instead of a parametric expression, a look-up table is used (see Fig. 4). Its data has been obtained from finite element analysis and experimentation (Ramirez-Laboreo and Sagues, 2018).

In Fig. 5, the desired position and its derivatives (z_{ref}, v_{ref}, a_{ref}) are displayed. Three additional useful signals are calculated and shown in Fig. 5: the required magnetic force (as described in Section 3.1), the required action u^*, and B_j. The required action is the absolute value of u to be able to track z_{ref} in an ideal scenario (no perturbations or errors),

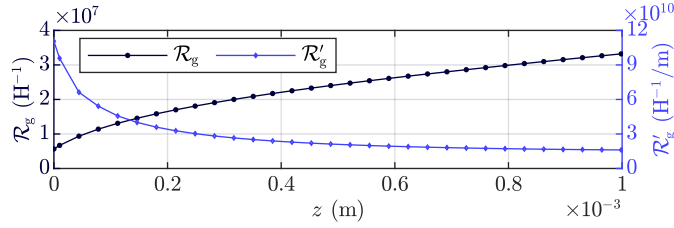$$u^* = \frac{|f_j - j_{\text{ref}}|}{|B_j|}. \tag{48}$$

Fig. 4. Gap reluctance and its derivative with respect to the gap length.

Note that, if $\tau_{\mathrm{mov}} = 3$ ms, F^*_{mag} is positive in a small interval in the breaking operation (around $t/\tau_{\mathrm{mov}} = 2$). Thus, this trajectory is infeasible. This can be checked as well in u^*, which tends to infinity as F^*_{mag} approaches zero. Then, as the motion duration increases, the requirements are less demanding, because v_{ref} and a_{ref} are reduced. Therefore, the maximum values of u^* are also reduced.

A necessary condition for convergence to $s = 0$ is $u_{\max} > \max(u^*(t))$. This condition is sufficient for perfect tracking in the ideal case, in which $\varepsilon = 0$. Otherwise, in general, a sufficient condition for convergence can be derived from (30),

$$u_{\max} \geq \max(u^*) + \frac{\max\left(|\varepsilon|\right) + \eta}{\min\left(|B_j|\right)}, \qquad (49)$$

where ε is bounded, assuming that $\tilde{v}$ and $\tilde{a}$ are bounded,

$$\max\left(|\varepsilon|\right) \leq \varepsilon\left(\max(|\tilde{v}|),\, \max(|\tilde{a}|)\right). \qquad (50)$$

Some assumptions must be made about the bounds of errors $\tilde{v}$ and $\tilde{a}$ to satisfy the previous condition. As an example, the controller constants are set as

$$\lambda_1 = \lambda_2 = 2000, \qquad \eta = 10^5. \qquad (51)$$

And, for the sake of simplicity, very conservative assumptions are made about the error bounds,

$$|\tilde{v}| \leq 0.2 \max(|v_{\mathrm{ref}}|), \qquad |\tilde{a}| \leq 0.2 \max(|a_{\mathrm{ref}}|). \qquad (52)$$

Thus, from (49) and (50), the robustness condition is $u_{\max} \geq 39.13$ V (if $\tau_{\mathrm{mov}} = 4$ ms), or $u_{\max} \geq 31.29$ V (if $\tau_{\mathrm{mov}} = 5$ ms). As expected, the condition is less restrictive when the motion duration is increased.

Note that, in order for the controller to be robust to modeling disturbances, the model parameters used to derive the robustness criteria (49) should represent the worst-case scenario, assuming the bounds of each model parameter are known. In practice, however, determining the combination of parameters that results in the worse-case scenario may be too cumbersome, due to the immense number of possibilities. Alternatively, a Monte-Carlo evaluation could be performed, permuting all parameters inside their bounds, and then selecting $u_{\max}$ such that (49) holds for every case.

4.2 Sampling rate analysis

We have proved that robustness can be guaranteed under some reasonable operating conditions. Still, the sampling rate may be a limiting factor, and its influence should be analyzed. Thus, the proposed controller is tested with different sampling periods T_{s}. As reference, the second position trajectory from Section 4.1 is used ($\tau_{\mathrm{mov}} = 4$ ms). The controller constants are set as in Section 4.1, with
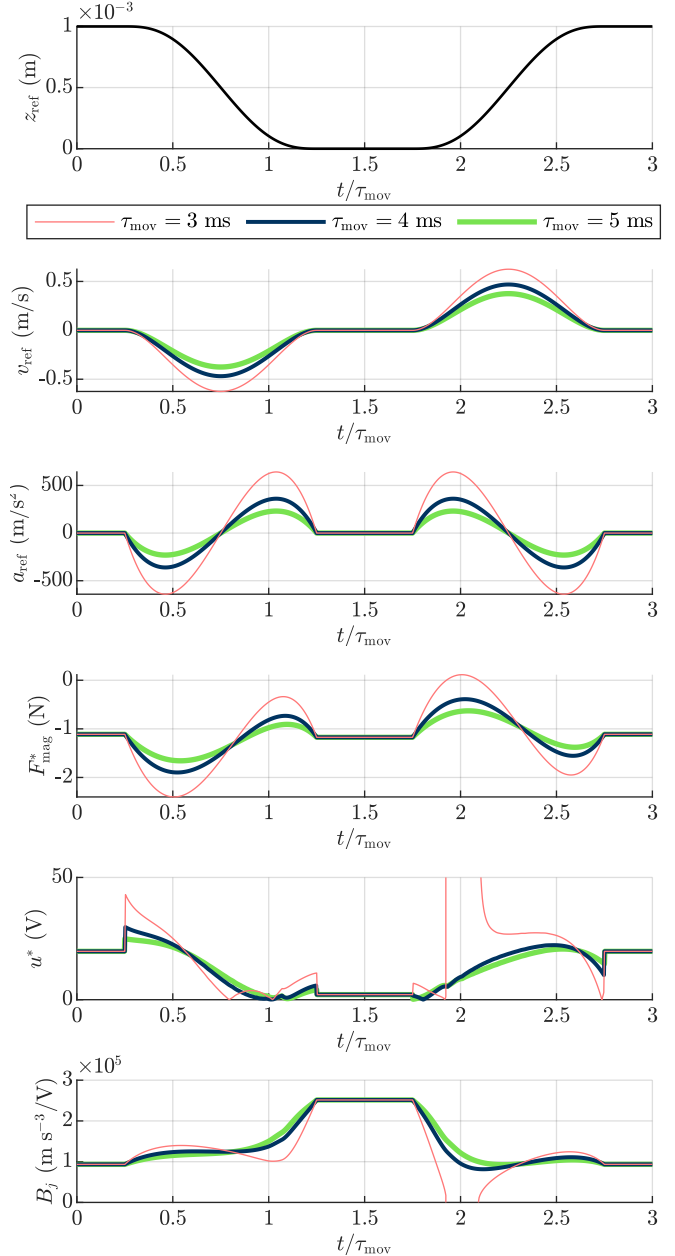

Fig. 5. Simulation results. Note that the time axis is normalized with respect to τ_{mov}.

$u_{\max} = 40$ V. The dynamic system is simulated using the hybrid automaton from Fig. 2 and the model parameters from Table 1.

The impact velocities are calculated for different sampling periods and depicted in Fig. 6, separating the making and breaking operations. With a sampling rate of 100 kHz, the results are very good, specially in the making operation. For larger sampling periods, the results increasingly worsen. Still, with a sampling rate of only 10 kHz, the impact velocities are better than the ones in a non-controlled scenario. For reference, using a square voltage of 40 V and 0 V, the impact velocities are -2.2 and 0.9 m/s, for the making and breaking operations respectively (which are beyond the graph limits).

Fig. 7 presents the resulting state variables for three representative sampling periods. With a sampling rate of
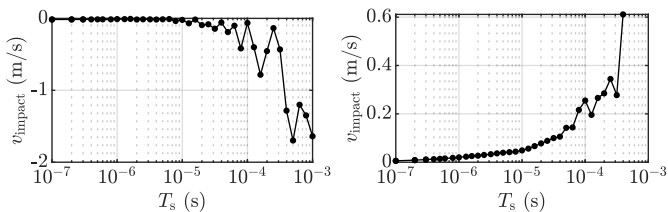
Fig. 6. Impact velocities in making (left) and breaking (right) operations, as functions of the sampling period.
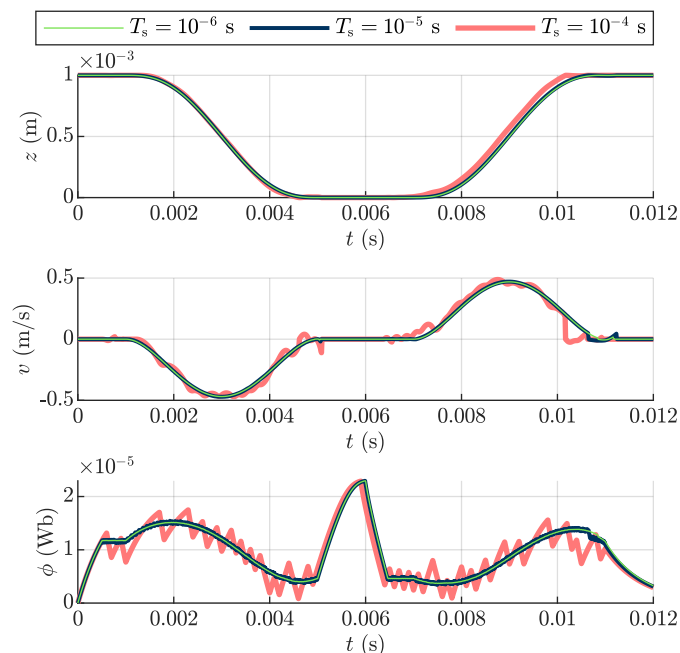

Fig. 7. Simulated state variables using the controller with three different sampling periods T_s.

1 MHz, the tracking is almost perfect. With a sampling rate of 100 kHz, there is a slight error in the position (almost imperceptible in the graphic), but the impact velocities are appreciably larger. Still, the performance is very good. With a sampling rate of 10 kHz, the results are much worse. The high ripple of the magnetic flux is filtered, but leads to significant tracking errors. Even though the position errors may seem small, the velocity errors and, more importantly, the impact velocities are much larger than in the other cases.

5. CONCLUSIONS

We have addressed the soft-landing control of single-coil reluctance actuators, presenting a sliding-mode controller which does not use any information about the dynamic system. We have also derived the convergence criteria, based on a generalized dynamical model. This controller requires to know the position and its derivatives, as well as the sign of ϕ. Alternatively, the current through the coil can be restricted to nonnegative values. That way, the magnetic flux is always nonnegative, simplifying the control.

Due to the fast dynamics, the sampling rate must be large enough to track the predefined position and achieve low impact velocities. Note that the position errors may be small with reasonably low sampling rates, but the resulting impact velocities are significant. Anyway, if a faster control cannot be implemented, the results are still better than in non-controlled scenarios.

In many devices the position is not measurable in real time. Thus, further investigation is required concerning the real-time position estimation from easily measurable signals, e.g. voltage and current, and the evaluation of the controller robustness with respect to estimation errors.

REFERENCES

Eyabi, P. and Washington, G. (2006). Modeling and sensorless control of an electromagnetic valve actuator. *Mechatronics*, 16(3), 159–175.

Kahveci, N.E. and Kolmanovsky, I.V. (2010). Control Design for Electromagnetic Actuators Based on Backstepping and Landing Reference Governor. *IFAC Proc. Vol.*, 43(18), 393–398.

Katalenic, A., Butler, H., and van den Bosch, P.P.J. (2016). High-Precision Force Control of Short-Stroke Reluctance Actuators with an Air Gap Observer. *IEEE/ASME Trans. Mechatronics*, 21(5), 2431–2439.

Lee, J.H., Yun, Y.W., Hong, H.W., and Park, M.K. (2015). Control of spool position of on/off solenoid operated hydraulic valve by sliding-mode controller. *J. Mech. Sci. Technol.*, 29(12), 5395–5408.

Levant, A. (1993). Sliding order and sliding accuracy in sliding mode control. *Int. J. Control*, 58(6), 1247–1263.

Moya-Lasheras, E., Ramirez-Laboreo, E., and Sagues, C. (2019). A Novel Algorithm Based on Bayesian Optimization for Run-to-Run Control of Short-Stroke Reluctance Actuators. In *2019 Eur. Control Conf.*, 1103–1109.

Moya-Lasheras, E., Sagues, C., Ramirez-Laboreo, E., and Llorente, S. (2017). Nonlinear bounded state estimation for sensorless control of an electromagnetic device. In *2017 IEEE 56th Annu. Conf. Decis. Control*, 5050–5055. IEEE.

Ramirez-Laboreo, E., Roes, M.G.L., and Sagues, C. (2019). Hybrid Dynamical Model for Reluctance Actuators Including Saturation, Hysteresis and Eddy Currents. *IEEE/ASME Trans. Mechatronics*, 24(3), 1396–1406.

Ramirez-Laboreo, E. and Sagues, C. (2018). Reluctance actuator characterization via FEM simulations and experimental tests. *Mechatronics*, 56, 58–66.

Ramirez-Laboreo, E., Sagues, C., and Llorente, S. (2016). A New Model of Electromechanical Relays for Predicting the Motion and Electromagnetic Dynamics. *IEEE Trans. Ind. Appl.*, 52(3), 2545–2553.

Slotine, J.J.E. and Li, W. (1991). *Applied Nonlinear Control*, volume 199. Englewood Cliffs, NJ: Prentice Hall.

Yang, Y.P., Liu, J.J., Ye, D.H., Chen, Y.R., and Lu, P.H. (2013). Multiobjective optimal design and soft landing control of an electromagnetic valve actuator for a camless engine. *IEEE/ASME Trans. Mechatronics*, 18(3), 963–972.

Zhao, X., Li, L., Song, J., Li, C., and Gao, X. (2016). Linear Control of Switching Valve in Vehicle Hydraulic Control Unit Based on Sensorless Solenoid Position Estimation. *IEEE Trans. Ind. Electron.*, 63(7), 4073–4085.